Food and Bioprocess Technology
https://doi.org/10.1007/s11947-024-03346-8

RESEARCH

Improving Gelling Properties of Tofu: Study on ApnA Aspartic Protease Enzyme Impact on the Resulting Chemical and Microstructure Properties

Fatma Ali[1] · Xuhui Liu[1] · Sabine Danthine[2]

Received: 25 July 2023 / Accepted: 20 February 2024

Abstract
This study investigated the prospective effect of ApnA enzyme under different concentrations (μL/100 mL soymilk) compared to chemical (pH, $MgCl_2$, and K-carrageenan, respectively) as tofu coagulants. The resultant tofu samples were analyzed for compositional analysis, thermal properties, water distribution, and microstructure properties. The higher concentration of enzyme used, the higher resulted moisture content of tofu. ApnA enzyme increased the cross-linking through protein molecules and trapped more water within the gel network. Tofu samples prepared by different concentrations of ApnA enzyme displayed significantly less freezable water content (15.44, 12.84, and 19.46 g/100 g). In particular, 800 μL ApnA/100 mL soymilk formed an interconnected gel matrix with regular distribution with almost invisible cavities. The thermal pretreatment and the increased coagulation time might encourage this irregular structure. On the other hand, the gel network coagulated using the reduction of pH showed a weaker gel due to an accelerated acidification.

Keywords Soy protein · Chemical coagulants · ApnA enzyme · Cross-linking

Introduction

Tofu, commercially known as bean curd, has a long history in China, dating back to the western Han Dynasty (202 BC to 8 AD). Originating from Asia, particularly in China, soybean products have gained global popularity as the most widely consumed vegan food item. The worldwide consumption of soy products has risen due to their exceptional nutritional value and associated health advantages (Wang et al., 2020). The addition of a coagulant is a crucial step in transforming soymilk into tofu curds. The coagulation properties of soymilk play a vital role in achieving high yields and desired texture of tofu (Stanojevic et al., 2020). Tofu coagulants are categorized as either mineral salts or acidic coagulants, depending on their chemical mechanisms. Nigari (NGR) and gypsum (GYP) are widely used traditional mineral salt coagulants in tofu production. However, both coagulants have notable drawbacks. NGR offers satisfactory organoleptic properties, but comes at a high cost, while GYP is cost-effective, but has inferior sensory properties. The higher cost of NGR is attributed to its complex production process, which involves seawater evaporation and sodium chloride removal (Joo & Cavender, 2020).

Mineral salt coagulants work by binding bivalent cations with deprotonated phosphate groups, an effective mechanism for soymilk production. This reaction leads to a decrease in pH. Hence, proper pH adjustment is essential during industrial processing, accomplished using mineral salt coagulants (Kanauchi et al., 2015). Certainly, exploring how pH variations could impact other time-related developments (such as alterations in texture and flavor) would hold significant relevance. pH values ranging from 6 to 10 (neutral and alkaline conditions) could potentially trigger changes in certain functional groups, resulting in the creation of more resilient molecules, particularly those containing amine functionalities. An array of substances, encompassing aromatic compounds (S1), sulfides, mercaptans, and thioethers (S3), terpene esters (S5), helium (S8), hydrocarbons (S10), and ethylene (S13), engaged with

✉ Fatma Ali
fatmaali@tust.edu.cn; alifatma.tust@gmail.com

[1] Department of Biological Chemical Engineering, College of Chemical Engineering and Material Science, Tianjin University of Science and Technology, TEDA, Tianjin 300457, China

[2] Food Science and Formulation, University of Liège-Gembloux Agro-Bio Tech, Gembloux, Belgium

Published online: 05 March 2024

the pH-adjusted solutions, lead to the emergence of novel aroma compounds. In turn, low-pH coagulants can impart an acidic taste to tofu and potentially alter its texture, making it less desirable for some consumers. The resulting tofu might be perceived as sour or tangy, which might not be appealing to everyone (Phuhongsung et al., 2020).

In their study, Zhang et al. (2019) examined the effects of okara and transglutaminase (TGase) on improving the quality and gel strength of high-fiber tofu. The addition of okara separately resulted in a decrease in gel strength compared to the control tofu sample. However, when okara was combined with TGase, the gel strength was significantly enhanced, more than doubling its strength. The presence of okara on its own weakened the gel strength due to the insufficient formation of protein, caused by the efficient insoluble fiber in okara. Conversely, TGase facilitated the formation of intermolecular ε (γ-glutamyl) lysine (Lys) bonds within the protein molecules, reinforcing the cross-linking of the gel matrix. Despite the assumption that the dietary fiber in okara could enhance water retention, the TGase-treated protein network exhibited a higher water-holding capacity (WHC) due to the strength of the protein cross-linking network.

The significance of aspartic proteases has been gaining attention in various industries, including food, beverage, fermentation, animal feed, and pharmaceuticals, due to their diverse applications (Song et al., 2020; Theron & Divol, 2014). These proteases have found utility in multiple areas, such as cheese production, bread dough systems, meat processing, acidic hydrolysis of fish proteins, correction of enzyme deficiency syndromes, protein degradation, and reducing turbidity in fruit juices (Theron & Divol, 2014). Despite their broad applicability in the food industry, the commercial availability of aspartic proteases is limited. Currently, commercially available aspartic proteases are typically mixtures of peptidases, resulting in complex reactions that can lead to protein degradation (Marangon et al., 2012).

Despite significant research conducted on soy and its various applications, there remain several challenges in tofu processing that require further investigation. Recent studies have highlighted both the advantages and drawbacks of the gel network formed through the use of chemical coagulants (Ali et al., 2021). However, the impact of biological methods, particularly enzymes, whether positive or negative, is still not well understood. In this particular study, our team isolated an enzyme from *Aspergillus niger*, identified as a potential aspergillopepsin-like aspartic protease (Song et al., 2020). Our team analyzed three aspergillopepsin-like aspartic proteases, examining their biochemical properties and potential applications in processes related to casein and soybean protein. The primary objective of this study was to investigate the effects of the ApnA aspartic protease enzyme on the resulting chemical and microstructural properties of tofu. The study focused on assessing the impact of the aspartic protease ApnA on the texture, yield, WHC, thermal stability, freezable water content, secondary protein structure, and microstructural properties of tofu. As interest in physical methods grows, a better understanding of alternative enzymatic cross-linking methods could contribute to improving the gel network of tofu, resulting in enhanced characteristics.

Materials and Methods

Materials

Soybean grains were purchased from a local supermarket in Tianjin, China. K-carrageenan and magnesium chloride 6-hydrate ($MgCl_2$. 6 H_2O) were obtained from Shanghai Macklin Biochemical Co., Ltd., Shanghai, China. Hexane (98%), methanol (99%), and potassium hydroxide (97%) were purchased from Sigma Chemical (St. Louis, MO, USA). All chemicals used in the trails were of reagent grade.

ApnA Enzyme Preparation

Aspergillus niger F0215 used in this study was isolated from a natural source, identified, and stored at the culture and information center for Industrial Microorganisms of China Universities (CICIM-CU), Tianjin University of Science and Technology, China (Niu et al., 2017). *A. niger* F0215 was grown in potato dextrose agar (PDA) medium (2% potato, 2% dextrose, and 1% agar) with 1% casein (Sigma, USA) at 32 °C and 240 rpm. After 24-h incubation, the mycelia were harvested for total RNA isolation. *Escherichia coli* JM 109 was grown in Luria–Bertani (LB) medium (10% tryptone, 5% yeast extract, and 10% NaCl) at 37 °C and used for cloning experiment (Song et al., 2020). *Pichia pastoris* GS115 was used for extracellular expression of the recombinant proteins and recombinants were cultivated according to the instructions manual from the supplier (Invitrogen, USA). *Pichia Pastoris* GS115 was grown in minimal liquid medium (YPG/YPD) containing (10 g/L yeast extract, 20 g/L peptone, and 20 g/L glycerol). The fermentation medium containing 4% glycerol was used for bacterial growth for about 18 ~ 24 h. Fermentation stage consumed 18 h, and then, 50% glycerol was added (containing 3 mL PTM1). Throughout the fermentation process, data was recorded every 2 h. During the methanol induction phase, samples were examined every 4 h to measure enzymatic activity. After the fermentation stage was fully completed, the fermentation broth was centrifuged to remove the bacteria and obtain the enzyme solution. The enzyme solution was stored at − 70 °C for 14 h and then freeze dried to obtain the enzyme powder (stored at − 20 °C for 4 weeks).

Tofu Manufacturing

Tofu was manufactured according to the method of Shen and Kuo (2017) with slight modifications on the coagulant types, pH, and concentrations. Soybeans (100 g) were washed and soaked in distilled water at a ratio of 1:3 (w/w) for 7 h at room temperature. After 7 h of soaking, same water ratio was added for another 7 h. The swollen soybeans were drained and the ground with distilled water (1:8, w/w) in food grinder. The ground soybeans were filtered using 120 mesh to separate okara from soymilk (800 mL approximately). The pH of soymilk was adjusted to 3 using hydrochloride acid and determined by a digital pH meter with a glass electrode. The whole quantity of raw soymilk was divided to 6 batches; all of them were heated in controlled water bath to 95 °C/5 min with regular stirring. Three batches of them were cooled down to 50 °C in an ice bath, and then the enzyme was added immediately at a ratio of 700, 800, and 900 µL/100 mL soymilk, respectively. The remaining three soymilk bathes were cooled to 85 °C and then were added of two of the coagulants (0.5 g/100 mL K-carrageenan–0.5 g/100 mL $MgCl_2$), while the last batch was adjusted to pH 3. The soymilk-coagulants suspension was mixed carefully at a speed of 320 rpm/20 s and then incubated for 20 min to form the curd. The curd was kept in a cheese cloth and placed in a wood press (12 cm × 8 cm × 3 cm). The tofu curd was pressed at 10 g/cm^2 for first 10 min and then 20 g/cm^2 for another 20 min to remove the whey. The resulting tofu was stored at 4 °C for 24 h for further analysis.

Texture Measurement

A TA.XT Plus Texture Analyzer was used to analyze the tofu texture (Stable Micro System, Goldaming, Surrey, UK) using a cylinder probe P36. The equipment parameters were set as follows: pre-test speed: 5.0 mm/s; test speed: 1.0 mm/s; post-test speed: 1.0 mm/s according to Cao et al., (2017). Tofu cubic samples, 3.6 cm in diameter and 2.0 cm in height, were compressed twice to 50% deformation. Hardness, gumminess, cohesiveness, and chewiness were obtained as tofu texture traits. This measurement was repeated 3 times for each sample.

Measurements of Syneresis, Yield, and Composition Analysis

Oven drying method and Kjeldahl method were utilized to determine the moisture and protein contents according to AOAC, (2000). Moisture content was calculated by drying 5 g of fresh tofu at 105 °C in an air oven to constant weight. Nitrogen to protein conversion factor is 6.38. The yield of tofu was calculated and expressed as the wet weight of tofu per 100 mL of soymilk following Rekha and Vijayalakshmi (2013) method. Tofu samples syneresis was measured according to Shen and Kuo (2014). Syneresis was expressed as the percentage of exuded liquid weight to the sliced tofu sample weight.

WHC

WHC was determined for tofu samples according to Cao et al. (2017), with slight modifications. Each sample (3 g) was cut into 5 × 5 × 5-mm cubes and centrifuged at 5632 g / 20 min at 4 °C in a H1850R high-speed refrigerated centrifuge (Cence Company, China). Resulting liquid was filtered and the remaining supernatant was collected and neglected. The water holding capacity was calculated using the following equation:

$$WHC = \left(W_t - W_r\right)/W_r \times 100\% \quad (1)$$

where W_t is tofu cubes weight before centrifuge and W_r is the weight of the resulted water after centrifuge. All measurements were calculated in triplicate per each sample.

Fourier Transform Infrared Spectroscopy (FTIR) Analysis

The second structure of tofu samples was analyzed according to Zheng et al. (2021) with slight modifications. Tofu samples were freeze-dried and then mixed with potassium bromide powder (1:100 w/w). A tableting equipment was used for samples compressing. All samples were scanned using a Thermo Nicolet IS50 FTIR spectrometer (VECTOR22, Brook instruments Inc., Germany) with an average of 32 scans at 4 cm^{-1} resolution from 4000 to 400 cm^{-1}.

A scanning band from 1700 to 1600 cm^{-1} was used to investigate the amide I band and the peak fit v4.12 derivatives software was used to obtain the second derivative spectra of the infrared spectra (Qi et al., 2017). The software was displayed 9 fit sub-peaks rely on an increase of the wavelength from 1700 to 1600 cm^{-1}. The major secondary structures (α-helix, β-turns, β-sheets, and random coils) were calculated from the sub-peak areas. Peaks 2, 3, 7, and 8 were β-sheets, peak 4 was random coil, peak 5 was α-helix, and β-turn was peak 6. Peaks 1 and 9 were unknown peaks rely on their wavelengths. Zheng et al. (2021) showed one unknown peak at wavelength 1615 cm^{-1} and our samples showed almost the same peak at 1617 cm^{-1} and another one appeared at wavelength 1693 cm^{-1}.

Thermal Properties and Water Distribution

The thermal properties of tofu samples were investigated using a differential scanning calorimetry (DSC-204F1,

NETZSCH, Germany). Tofu samples were weighed (5–10 mg) into an aluminum pan, that was sealed, and heated from 20 to 120 °C at a rate of 2 °C/min. An empty pan was used as a reference.

Freezable water content of prepared tofu samples was measured using the same DSC equipment, but with different parameters. Samples (5–10 mg) were heated from − 60 to 50 °C at 5 °C/min. The onset, end set temperature, the melting enthalpy (ΔH), peak temperature, peak width, and peak intensity were analyzed by NETZSCH Proteus Thermal Analysis v5.2.1 software, NETZSCH, Germany. Freezable water content (FW) was calculated using the following equation according to Wang et al., (2014a, b):

$$FW\ (g/100g) = \left(\Delta H/\Delta H_w\right) \times 100 \quad (2)$$

where ΔH is the melting enthalpy of sample and ΔH_w is the enthalpy of water (335 J/g). All the measurements were performed in triplicate per each sample.

Fluorescence

The fluorescence spectrum of tofu samples was investigated using a F-7100 fluorescence spectrophotometer (Hitachi) according to Zheng et al. (2021), with some modifications.

About 0.2 g of sample powder was compressed by the solid sample holder (5J0-0152), which optimized the measurement of powder samples and prevented the specular reflection from the sample surface. An excitation wavelength of 280 nm, a scanning speed of 1200 nm/min, and an emission spectrum from 300 to 500 nm were used for 2D spectrum test. The emission spectrum range of 200–500 nm, voltage ranged from 450–400 V, with scanning speed of 30,000 were used for 3D condition test.

Curd Microstructure

Scanning electron microscope (SEM) images of tofu samples were obtained using a SU-1510 Scanning Electron Microscope (Hitachi Ltd., Japan) with an accelerated voltage of 10 kV. Samples were cut into 3 × 3 × 1-mm cubes and freeze-dried according to Sun et al. (2019) with slight modifications. Tofu pieces (2 × 2 × 1 mm) were washed twice using 2.5% glutaraldehyde solution (prepared in 0.1 M phosphate buffer, pH 7.4). Subsequently, different ethanol concentrations (50, 70, 90, and 100%, respectively, for 15 min each concentration) were added to the treated tofu samples for dehydration. Afterwards, samples were immersed in ethanol and tert-butanol mixture (1:1, v/v) for 15 min and then dipped into 100% tert-butanol for further 15 min.

Results and Discussion

Tofu Yield, Syneresis, and WHC

The yield and composition of tofu samples produced from pH3, $MgCl_2$, K-carrageenan, and different concentrations of ApnA enzyme are shown in Table 1. The yield of ApnA700 tofu sample was higher than that of ApnA800 and ApnA900 samples. In general, ApnA700 tofu sample produced higher yield than that of other tofu samples produced from chemical coagulants. An increase of ApnA tofu samples yield was offset by a decrease in the moisture contents significantly compared to the remaining samples. The higher concentration of enzyme used, the higher resulted moisture content. In turn, the highest protein contents were observed significantly from ApnA tofu samples. Our findings resulting from coagulants were in correspondence with Cao et al. (2017) and Shen and Kuo (2017).

Typically, the protein molecules cross-linking is associated with the rise or reduction of syneresis values. The differences in the coagulant types used in this study led to significant diversities in the resulted syneresis outcomes as are displayed in Table 1. The coagulated tofu using polysaccharide demonstrated the highest syneresis value (2.48%), while the addition of $MgCl_2$ reduced syneresis by 0.71%. Regardless of the slight differences

Table 1 Yield, composition, syneresis, and water holding capacity of tofu samples

Treatment	pH3	$MgCl_2$	K-car	ApnA700	ApnA800	ApnA900
Protein (%)	11.14 ± 0.15^{f}	12.43 ± 0.23^{e}	12.81 ± 0.18^{d}	13.11 ± 0.21^{c}	13.67 ± 0.29^{b}	13.96 ± 0.23^{a}
Crude fat (%)	3.39 ± 0.23^{f}	4.77 ± 0.21^{a}	4.63 ± 0.29^{b}	4.57 ± 0.17^{c}	4.29 ± 0.26^{d}	4.02 ± 0.21^{e}
Ash (%)	1.88 ± 0.07^{a}	1.71 ± 0.04^{f}	1.78 ± 0.17^{e}	1.85 ± 0.09^{b}	1.84 ± 0.05^{c}	1.82 ± 0.03^{d}
Moisture (%)	79.15 ± 0.75^{c}	80.69 ± 0.95^{b}	81.31 ± 0.92^{a}	69.43 ± 0.73^{f}	70.12 ± 1.05^{e}	71.90 ± 0.92^{d}
Yield	148.19 ± 1.43^{c}	110.31 ± 1.03^{f}	193.39 ± 1.27^{b}	211.73 ± 1.72^{a}	139.19 ± 1.64^{d}	125.06 ± 1.28^{e}
Syneresis (%)	1.85 ± 0.03^{b}	1.77 ± 0.02^{c}	2.48 ± 0.04^{a}	1.60 ± 0.02^{f}	1.61 ± 0.02^{e}	1.69 ± 0.03^{d}
WHC (%)	66.83 ± 1.04^{e}	63.16 ± 1.38^{f}	71.45 ± 1.93^{d}	76.26 ± 1.04^{c}	79.63 ± 1.08^{a}	77.28 ± 1.21^{b}

*All values shown are means ± standard deviation ($n = 3$)

*Different lowercase letters within the same rows are significantly different ($P < 0.05$)

in syneresis values among tofu samples produced from ApnA, more water was trapped in interstitial parts of the tofu gel compared to the remaining samples. Most probably the chemical coagulants formed a quicker gel network, leading to a coarse net structure and less water being retained. ApnA enzyme increased the cross-linking through protein molecules and trapped more water within the gel network. Besides, we hypothesized that the protein cross-linking would persist during the storage period. This study outcome related to chemical coagulants is in accordance with Li et al. (2015), who reported an increase of syneresis value by the addition of carrageenan rather than $MgCl_2$.

WHC is an indicator of protein- water interaction through gel formation stage (Li et al., 2015). The premier stage of heat treatment at 95 °C led to elevated SH group levels as a consequence of β-conglycinin and glycinin denaturation (Tang, 2007). The addition of ApnA enzyme to the protein network in the presence of heat may weaken this feature and minimize the breakdown of SS bridges among acid and polypeptides of glycinin. On the other hand, providing ApnA to soymilk minimized the chances of alteration in the second structure during heating, which is an indicator of ApnA's capability for conformational rearrangement of protein inhibition (Zhang et al., 2019). Since the water holding capacity of ApnA samples were higher compared to other samples prepared from chemical coagulants, the coupled gel network ApnA-proteins could bind more water, as evidenced by increasing the yield and moisture content of ApnA tofu samples.

On the other hand, a more rigorous heat treatment is essential for unfolding the protein molecules due to their lower contact area in the native state compared to the unfolded state. Once unfolded, the protein molecules expose their hydrophobic sites, leading to intensified hydrophobic interactions caused by excluded volume effects. Consequently, the unfolded protein molecules become more susceptible to aggregation, which enhances the gel's ability to withstand puncture and compression (Zhao et al., 2016). The observed WHC of ApnA enzyme samples may be attributed to a higher concentration of cosolutes getting trapped within the gel's interstitial spaces, thereby entrapping more water within the gel. This outcome is in accordance with Qin et al. (2017) who induced soy protein isolate by TGase at various ultra-high pressures pretreatment. In that study, the protein unfolding promoted the TGase-induced reaction and led to stable uniformity and density in the gel network structure. Additionally, the uniform and dense microstructure might bind water in the protein gels, contributing to the reinforcement of WHC and gel strength.

Tofu Texture

The current study investigated the texture characteristics of tofu samples for their great importance in affecting the final quality of the product. Texture characteristics are divided into hardness, springiness, cohesiveness, and chewiness as are displayed in Fig. 1. Previous literature associated hardness and springiness values with the maximum force of the first compression and the rate of detected height distance divided by the original compression distance, respectively (Zheng et al., 2019). In the present study, tofu samples from different coagulants and various concentrations of ApnA enzyme showed significant differences ($P < 0.05$) in hardness and springiness values. Specifically, ApnA800 sample showed the highest hardness and springiness values, while the hardness and springiness values of pH3 sample were the lowest. The resulting differences in the structure of amino acids and the secondary structure markedly affect the structure of the obtained protein network. Therefore, a stable 3D protein network is produced through the formation of disulfide bonds within the coagulation stage. Based on that, ApnA sample may have more 11S sub-units than that of other samples.

Phuhongsung et al. (2020) demonstrated elevated hardness at low pH levels. Their findings align with our assertion that ApnA diminishes protein precipitation, leading to a more relaxed network structure as opposed to the initial densely packed protein matrix. The hardness outcome is in agreement with Zheng et al. (2021), who reported an increase of hardness with increasing the sulfur amino acid content, β-sheets structure, and 11S:75 ratios. ApnA800 sample displayed the highest hardness and springiness with highest β-sheets, stable 3D protein network, and stronger resistance to deformation. In turn, pH3 and $MgCl_2$ samples showed opposite values.

In terms of cohesiveness, ApnA900 condition exhibited a relatively high value, signifying strong intermolecular interactions. On the other hand, chewiness values displayed distinct patterns. ApnA700 exhibited an exceptionally high chewiness, possibly due to its unique texture. K-car and ApnA700 showed comparable chewiness values, indicating a potential similarity in texture. These variations in cohesiveness and chewiness highlight the diverse textural characteristics of the samples, emphasizing the importance of these parameters in understanding the material properties and potential applications. Further investigation into the underlying mechanisms governing these textural differences would provide valuable insights for optimizing product formulations or processes.

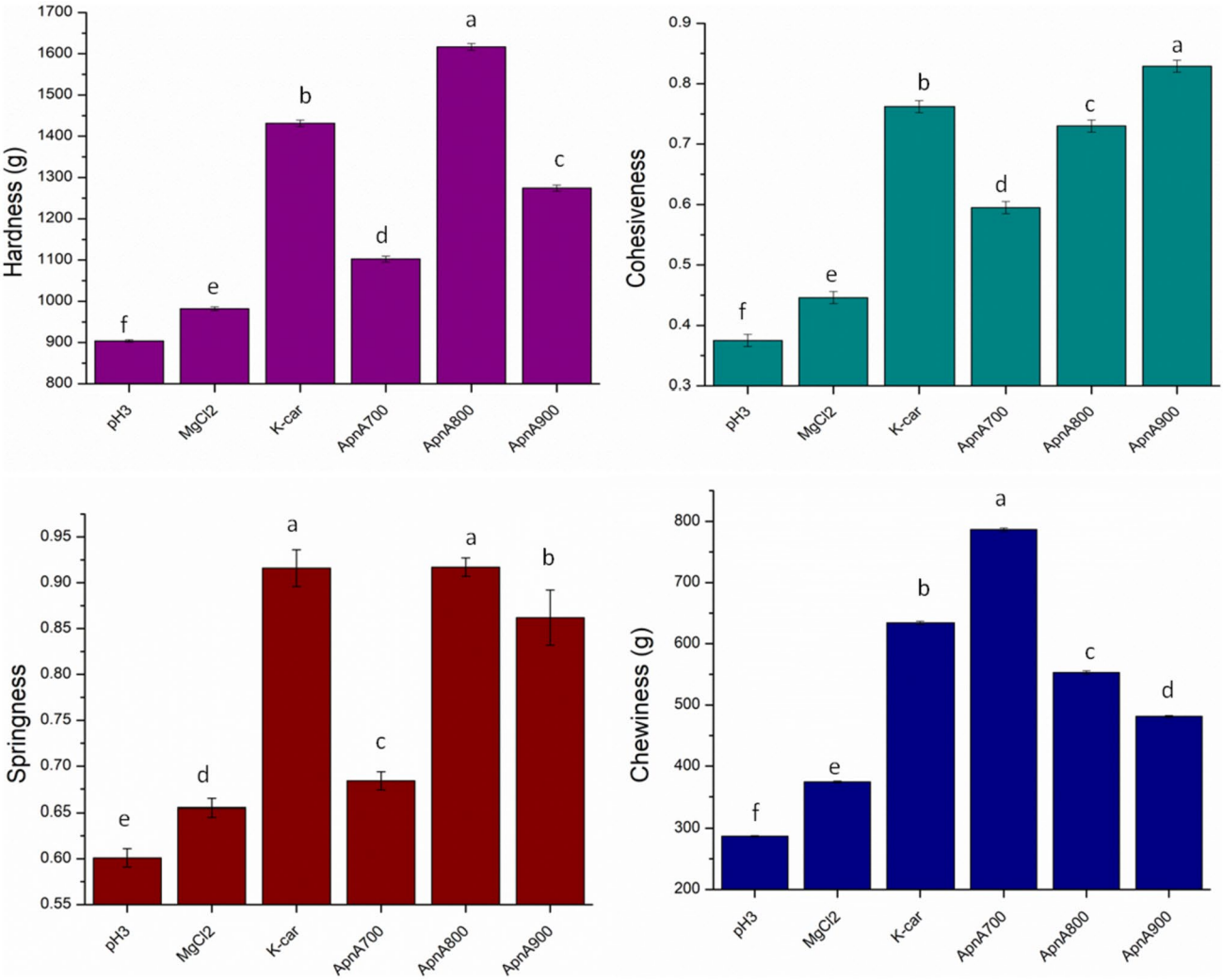

Fig. 1 Effect of different concentration of ApnA-enzymes on texture parameters

Thermal Stability

DSC profile is a key indicator of the denaturation temperature and enthalpy (ΔH). Investigating the denaturation behavior of soy protein is considered as one of the most substantial factor influencing the gel network structure, thus the resulting tofu final properties (Wang et al., 2014a, b). The thermal stability of tofu protein was investigated by determining the thermal function properties of ApnA, pH, $MgCl_2$, and K-car-treated tofu as shown in Fig. 2 and Table 2. No typical endothermic peaks were observed in the heat flow signals of tofu samples. In tofu protein, the most important endothermic peaks are those related to native β-conglycinin and glycinin, which occur at the denaturation temperature (T_d) of 70 °C and 90 °C, respectively (Brishti et al., 2017). The absence of these peaks was an indication of the complete denaturation of the protein after this thermal treatment. Our data are in correspondence with previous literature which reported the complete denaturation of native β-conglycinin and glycinin after the pretreatment at 90° or even higher (Ingrassia et al., 2019). The presence of high proportions of protein hydrophilic residues was probably the main reason for high T_d values, which disappeared up to 120 °C (Tang, 2007). Besides, higher T_d value was associated with a higher thermal stability of protein (Ibrahim et al., 2021).

In the present study, values of thermal properties were in agreement with the results of Ibrahim et al. (2021), who linked the high thermal stability to the degree of oil absorption capacity. A lower oil absorption capacity in pH, $MgCl_2$, and K-car treated-tofu samples resulted in producing more heat stable characteristics. In turn, the existence of some oil granules in ApnA-treated tofu samples, which observed in SEM results, reduced their thermal stability somewhat.

However the coagulation process temperature of pH, $MgCl_2$, and K-car-treated tofu samples (80 °C) was higher

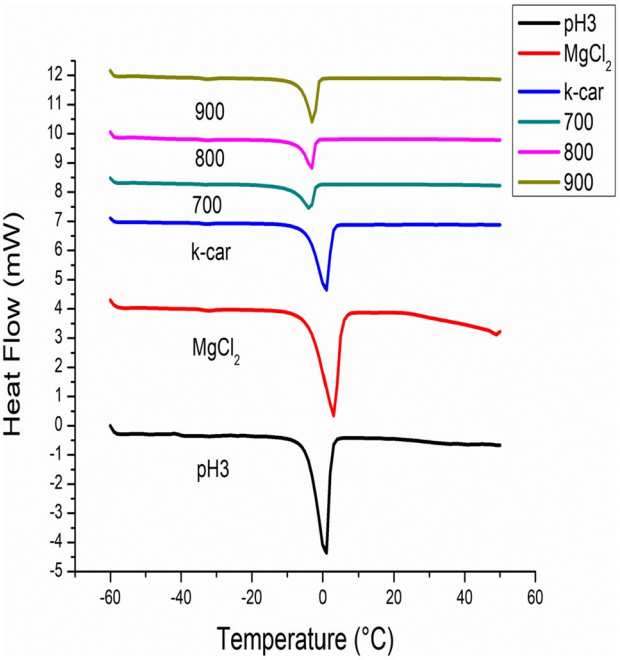

Fig. 2 DSC melting patterns of tofu samples as affected by pH3, $MgCl_2$, K-carrageenan, and various ApnA enzyme concentrations

than that of ApnA-treated tofu samples (50 °C), and ApnA800 sample showed non-typical endothermic peaks. The only reasonable explanation is that, during the long coagulation process, some hydrophilic interactions occurred among proteins and formed protein aggregates and some conglomerates, and most probably the DSC equipment translated it as a denaturation signals.

Freezable Water Content

The investigation of water distribution and mobility in polymer systems is one of the most important factors that give a strong indication of the resulting gel structure and stability. The efficient water distribution of tofu samples can be estimated from DSC that was used in this study. The possibility of water molecules binding to proteins negatively affected the properties of gel systems (Cao et al., 2017). This study investigated the water state in enzyme treated-tofu and other coagulant treated-tofu by measuring the freezable water content as is shown in Fig. 3. Tofu samples prepared by different concentrations of ApnA enzyme displayed significantly less freezable water content (15.44, 12.84, and 19.46 g/100 g, respectively) than that of tofu manufactured by pH3, $MgCl_2$, and k-car (63.43, 73.76, and 37.64 g/100 g, respectively). ApnA800 showed the lowest freezable water content significantly ($P < 0.05$) compared to other samples. The manufacture of tofu using $MgCl_2$ and low pH led to a complete lack of binding of water molecules and resulted in a large proportion of freezable water content in the gel network. This result is consistent with WHC result, which supported their inability to form a cross-linked molecule network. In turn, ApnA reduced the hydrophilic-group interactions; the water molecules bonded tightly, and formed a cross-linked molecular network of all the studied concentrations. The outcome from this study is in agreement with Cao et al. (2017), who correlated the higher WHC with low FW and higher tightness in the underlying gel structure.

A possible reason for the low content of FW in the enzyme-processed tofu samples can be related to the protein's stabilization in the aqueous phase. The presence of protein in the aqueous state without coalescence as a result of possible hydrophilic interactions positively affect the increase of sample stabilization and decrease FW content (Ghosh et al., 2006). ApnA enzyme may induced a steric stabilization against coalescence of unabsorbed proteins among two protein-covered surfaces. This reasonable argument was in accordance with Carpenter and Crowe (1988), who reported an increase of stability through freeze-thawing of enzymes with elevating the enzyme concentration. On the other hand, large ice crystals formation through freezing stage rely on the percentage of glycosylated proteins in the aqueous phase, which most likely decreased significantly with enzyme usage. As a consequence of enzyme action shortage found in this study, further experiments

Table 2 Thermal properties of the manufactured tofu samples

Tofu samples	Onset (°C)	End set (°C)	ΔH (J/g)	Peak (°C)	Width (°C)	Intensity
pH3	-4.4 ± 0.3^{c}	2.2 ± 0.3^{c}	-212.5 ± 2.6^{e}	0.7 ± 0.1^{c}	4.6 ± 0.7^{d}	4.02 ± 0.6^{a}
$MgCl_2$	-3.7 ± 0.6^{a}	4.9 ± 0.8^{a}	-247.1 ± 4.5^{f}	4.9 ± 0.6^{a}	6.1 ± 0.3^{a}	3.60 ± 0.4^{b}
K-car	-4.2 ± 0.2^{b}	2.5 ± 0.1^{b}	-126.1 ± 3.8^{d}	0.9 ± 0.1^{b}	4.8 ± 0.2^{c}	2.24 ± 0.5^{c}
ApnA700	-8.1 ± 0.7^{f}	-2.2 ± 0.3^{e}	-51.74 ± 2.5^{b}	-3.6 ± 0.1^{f}	4.9 ± 0.2^{b}	0.85 ± 0.1^{f}
ApnA800	-6.2 ± 0.4^{e}	-2.2 ± 0.1^{e}	-43.01 ± 1.7^{a}	-3.3 ± 0.2^{e}	3.3 ± 0.1^{f}	1.04 ± 0.1^{e}
ApnA900	-5.8 ± 0.3^{d}	-1.4 ± 0.2^{d}	-65.2 ± 2.6^{c}	-2.7 ± 0.4^{d}	3.5 ± 0.2^{e}	1.56 ± 0.1^{d}
STD						

*All values shown are means ± standard deviation ($n = 3$)

*Different lowercase letters within the same columns are significantly different ($P < 0.05$)

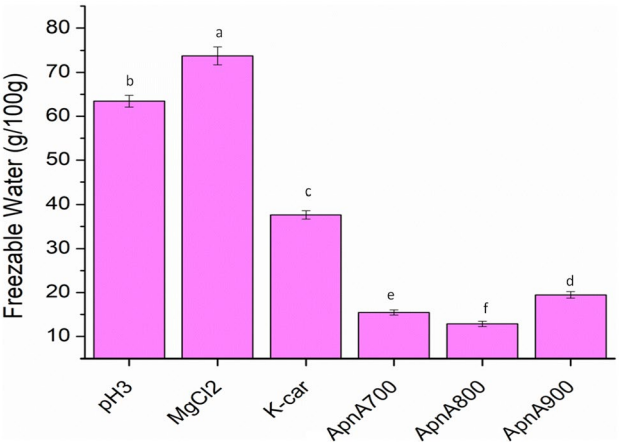

Fig. 3 Water distribution of enzyme treated-tofu and other coagulants-treated tofu samples

are needed to investigate the relative importance of ApnA enzyme on freeze–thaw stability of tofu samples. Nevertheless, this study showed the high effectiveness of ApnA enzyme on tofu thermal stability and properties.

FTIR

FTIR spectrum distinguished the chemical interactions and the second structure formed between proteins and lipids of tofu samples as is shown in Fig. 4. All tofu samples showed peaks at 2925 and 2854 cm^{-1}, no differences observed in these two peaks intensities among the samples with different treated coagulants. Amide-B (2923 $cm^{-1)}$ is commonly reflecting the interaction of $–NH_2$ groups through the peptide chain (Xue et al., 2019). As shown from the spectrum peaks, a minor shift in peaks of amide-B was noticed. Previous literature confirmed the correspondence of the absorbance band at 2852 cm^{-1} to C-H stretching vibration in aliphatic and aromatic compounds (Masek et al., 2014). From this point of view, it can be clarified that the aliphatic and aromatic compounds were not affected in the studied samples.

Millard reactions may increase or decrease the nutritional properties of protein food products (Sun-Waterhouse et al. (2014). Determining the effects of the treatments used on Millard reaction usually by studying the C = N stretching vibration between protein and polysaccharides. The coagulants used in this study affected the Millard reaction

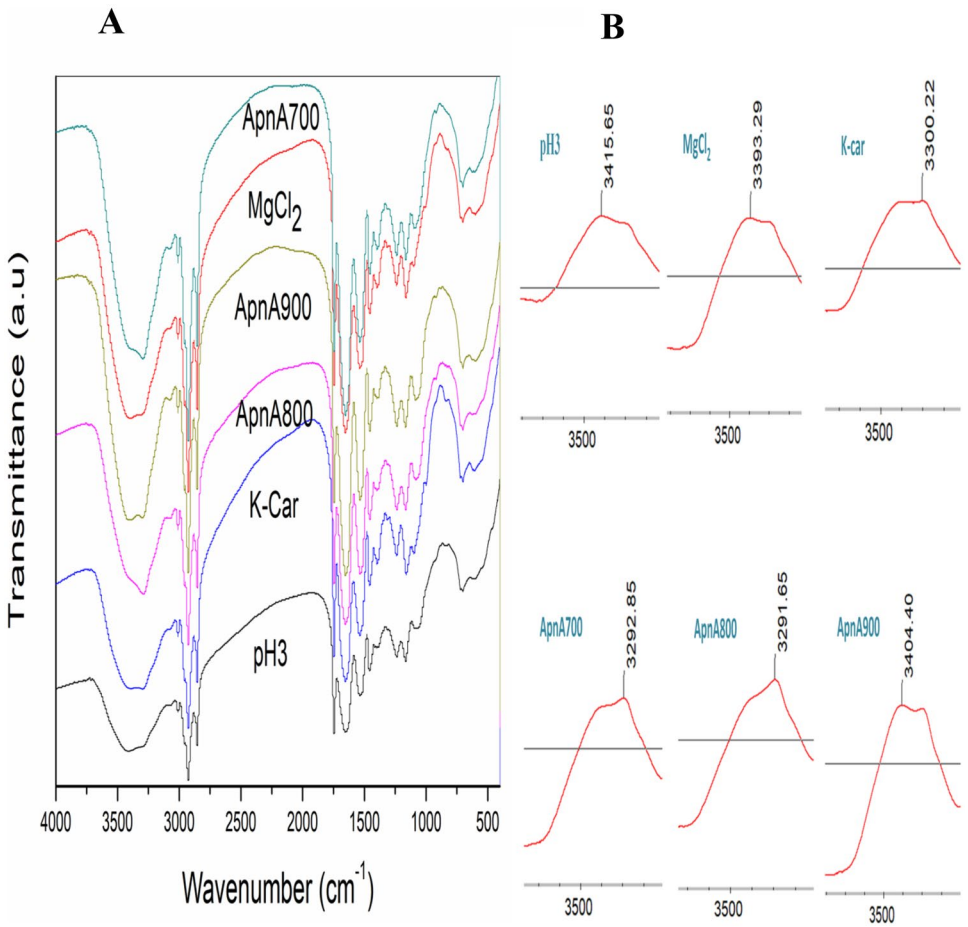

Fig. 4 **A** Fourier transform infrared spectroscopy of treated-tofu samples. **B** The differences in the tertiary structure of tofu samples using the fluorescence spectroscopy 3D analysis

through the occurrence of minor shifts in amide-I and amide-II peaks. Most likely the coagulants used including ApnA enzyme were unable to reduce the interaction between protein and polysaccharide during the pre-heat treatment. The absorbance peak at 1744 cm^{-1} corresponds to C = O vibration in fat which expressed lipid oxidation of soy oil. At elevated temperature, proteins have wide chance for cross-linking due to aldehyde and ketone functional groups existence, therefore lipid oxidation occurs (Carpin´e et al., 2016). No differences observed in 1744 cm^{-1} peak among all tofu samples, might be due to the low percentage of fat, not the effectiveness of the coagulants. On the other hand, the unique lipid absorption band appears exclusively at 1744 cm^{-1}, indicating the stretching of the C = O bond in the ester group of triglycerides and phospholipids (Premjit & Mitra., 2021).

The amide I band was deconvoluted into fit 9 sub-peaks using omnic software rely on an increase of the wavelength from 1700 to 1600 cm^{-1} as shown in Fig. 5. Wang et al., (2014a, b) determined the ranges of each second structure

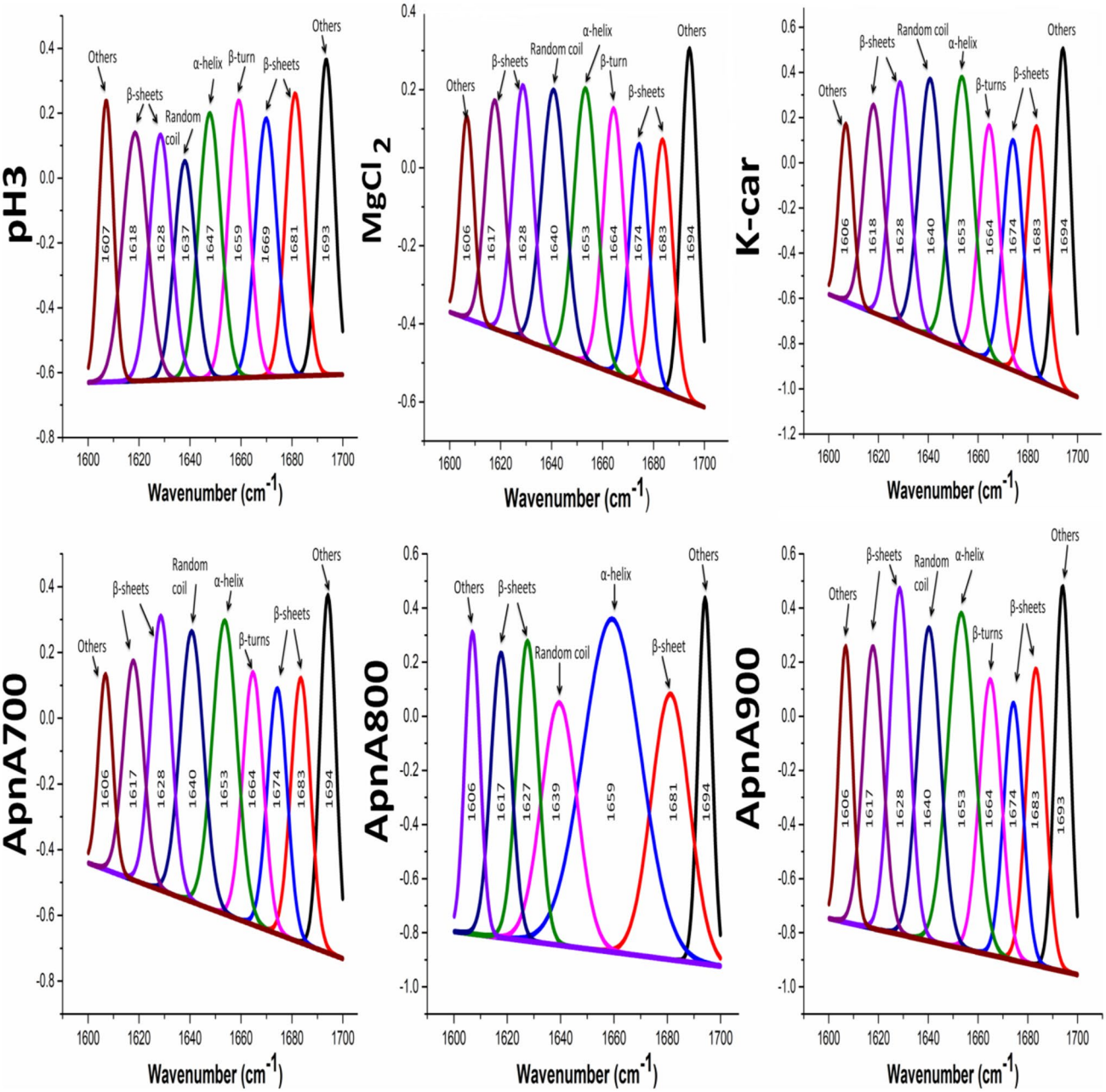

Fig. 5 Curve-fitted sub-peaks spectrum and deconvoluted spectrum of tofu samples prepared from pH3, $MgCl_2$, K-carrageenan, and ApnA enzyme

as follows: 1618–1640 cm^{-1} and 1670–1690 cm^{-1} related to β-sheets structure; nearly 1645 cm^{-1} for random coil; 1650–1660 cm^{-1} for α-helix; and 1660–1670 cm^{-1} for β-turn structure. Depending on these evaluated peaks of each secondary structure, the relative contents of secondary structure were calculated as displayed in Table 3. Notably, the prevalence of β-sheets stands out as a key determinant, with significant variations observed among different samples and this result was in agreement with Zheng et al. (2021). Tofu produced using ApnA at a concentration of 800 µL/100 mL soymilk exhibits a remarkable increase in α-helix content, reaching 20.17%, and a substantial elevation in β-sheets, accounting for 59.89%. This marked shift in secondary structure components corresponds to a significant enhancement in tofu hardness, consistent with established literature associating higher β-sheets percentages with increased gel firmness. In contrast, tofu samples coagulated with pH3, $MgCl_2$, and K-car demonstrate comparable α-helix and β-sheets percentages, suggesting a commonality in their structural profiles. Additionally, the absence of β-turns in the ApnA800 sample raises intriguing questions about the specific conformational changes induced by ApnA at this concentration. Overall, the secondary structure analysis provides nuanced insights into the molecular characteristics of tofu, offering a foundation for understanding and optimizing textural properties in tofu production. Further research could explore the mechanistic details behind the observed variations in secondary structure and their direct impact on tofu quality (Gao et al., 2015; Su et al., 2015; Zhang et al., 2016).

Fluorescence Spectroscopy

Protein denaturation and hydrophobic interactions are key factors that cannot be ignored for the stabilization of the tertiary structure and protein-protein interactions. Heat treatment is one of the important factors of protein denaturation and an increase of the surface hydrophobicity. Previous studies reported that the surface hydrophobicity of 7S and 11S globulins of soy protein fractions increased by heating and high-pressure treatment, particularly above 70 °C (Zhang et al., 2003). The 2D fluorescence intensity of tofu-chemical coagulants and tofu-ApnA enzyme samples are displayed in Fig. 6A. The usage of chemical coagulants and a concentration of 800 of ApnA enzyme increased the fluorescence intensity sharply, but a concentration of 700 and 900 of enzyme yielded a decrease in fluorescence. These results indicated that chemical coagulants are a transition coagulants to some protein fractions, which completely or partially denatured under the effect of these chemicals. Under the concentration of 700 of ApnA, less intermolecular interactions occurred and therefore less number of hydrophobic regions was exposed to heating. Another possible explanation is the transformation of protein fractions into a slightly different conformation, which in turn reduces the protein fractions exposure to denaturation (Zhang et al., 2005).

The differences in the tertiary structure of tofu samples are illustrated using the fluorescence spectroscopy 3D analysis and are shown in Fig. 6B. This analysis is used to determine the endogenous of proteins using the chemical environment of the fluorescence amino acids. For instance, Trp, Tyr, and Phe with relative fluorescence intensity ratio of 100:9:0.5, respectively (Xu et al., 2018). The transfer of energy from a Tyr to a Trp in most of globulins leads to an increase in Trp residues. This hypothesis govern that tofu samples prepared from chemical coagulants consist mainly of Trp unlike the other tofu-ApnA samples. Vivian and Callis (2001) divided the state of Trp residue into two states: polar and non-polar states rely on the emission peak (λ_{max}). An increase of the emission peak (λ_{max}) greater than 330 nm at 280 nm of excitation indicates a polar state of Trp residue as a result of combustion. In turn, a non-polar state is achieved when the emission peak (λ_{max}) is less than 330 nm at 280 nm. In this study, the fluorescence spectra of all the samples were dissimilar and higher than 330 nm. Therefore, authors fixed the emission peak (λ_{max}) of all samples at 400 nm at 280 nm for an accurate comparison at the same wavelength. Tofu samples prepared from chemical coagulants and ApnA-enzyme were in polar state of Trp residue with varying degrees and ApnA700 sample was the most polar, while pH3 sample was the least polar.

Table 3 Second structure of the different manufactured tofu samples

Sample	α-Helix (%)	β-Sheets (%)	β-Turns (%)	Random coil (%)
pH3	14.27 ± 0.2^{d}	57.16 ± 1.02^{b}	14.37 ± 0.04^{b}	14.19 ± 0.03^{b}
$MgCl_2$	14.29 ± 0.01^{c}	57.11 ± 1.3^{c}	14.39 ± 0.02^{a}	14.19 ± 0.01^{b}
K-car	14.30 ± 0.02^{b}	57.11 ± 0.7^{c}	14.39 ± 0.01^{a}	14.18 ± 0.05^{c}
ApnA700	14.30 ± 0.1^{b}	57.11 ± 0.5^{c}	14.39 ± 0.03^{a}	14.18 ± 0.06^{c}
ApnA800	20.17 ± 0.03^{a}	59.89 ± 1.1^{a}	NP	19.93 ± 0.02^{a}
ApnA900	14.29 ± 0.02^{c}	57.11 ± 0.9^{c}	14.39 ± 0.02^{a}	14.18 ± 0.04^{c}

*All values shown are means ± standard deviation ($n = 3$)

*Different lowercase letters within the same columns are significantly different ($P < 0.05$)

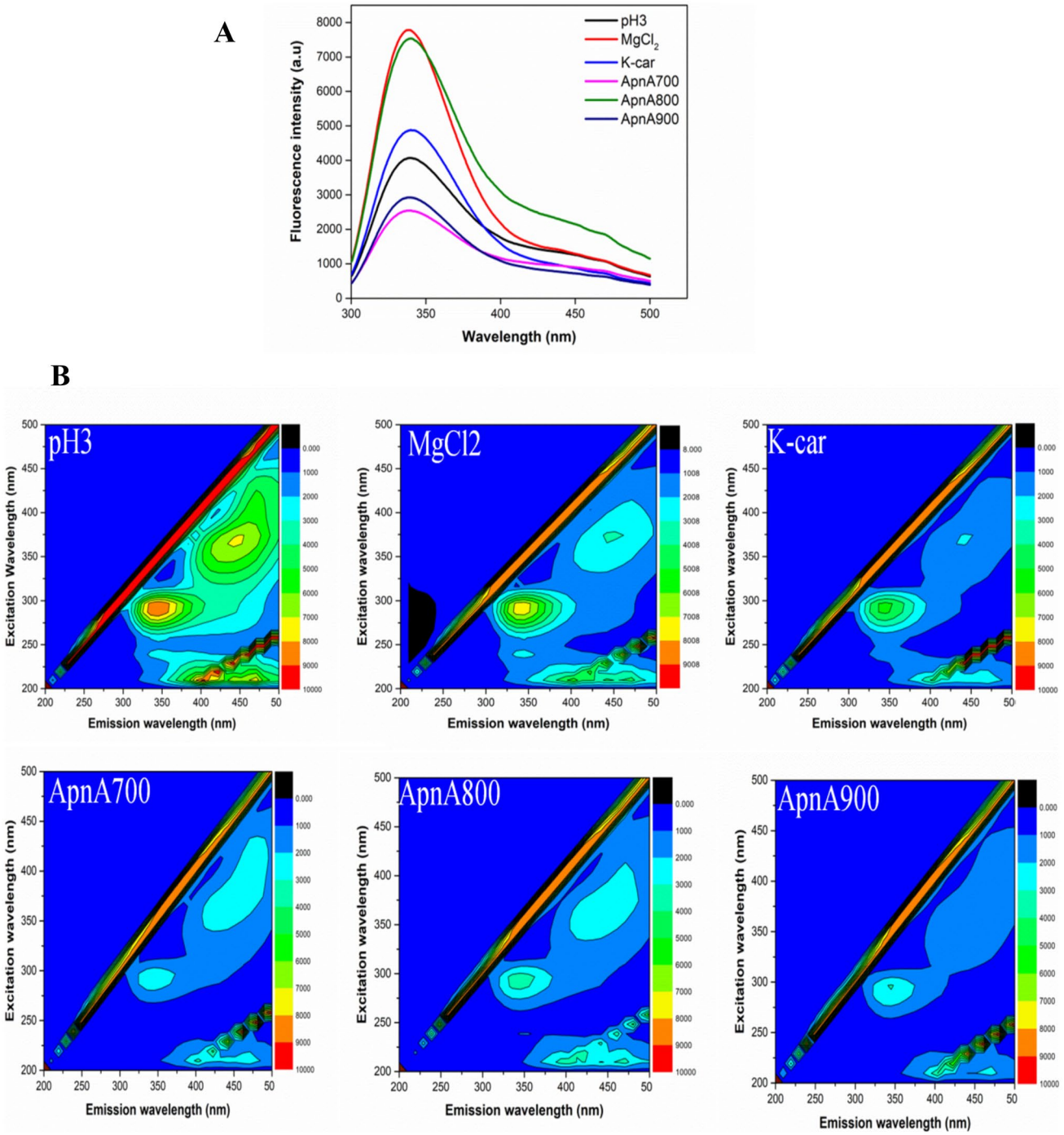

Fig. 6 **A** Two-dimensional fluorescence of different tofu samples. **B** Three-dimensional fluorescence of different tofu samples

Besides, there was no second peak for ApnA700 sample and this result indicated that tofu prepared from ApnA700 has a more flexible texture, in contrast to other samples including other ApnA800 and 900 samples. Relying on Kasha's principle, the position and shape of the emission spectrum are independent of the excitation wavelength, whereas the excitation yield is derived mainly from the lowest excitation singlet state (Zheng et al., 2019). In this study, the fluorescence intensity of all tofu samples was not consistent with the emission wavelength results, except for ApnA700 sample. This outcome supports Li et al.'s (2019) findings, who reported that the fluorescence intensity 3D's peak is due to the emission of the main chain of the protein peptide, and contradicts with Zheng et al. (2021), who showed that peak 2

is due to a higher excited state of the aromatic residue. This point in particular needs further investigation to determine the validity of both possible explanations.

Curd Microstructure

Scanning electron micrographs were captured to observe the changes of physiochemical properties of enzyme and chemicals induced tofu after the thermal treatment and coagulation process as shown in Fig. 7. Tofu samples produced under pH3, $MgCl_2$, and K-carrageenan treatments showed some cavities with dense structure. In turn, the overlapping structure observed in ApnA samples formed with lower density. Most probably the particle size of the coagulants added affected the size and the distribution of the resulting cavities (Ullah et al., 2019). On the same line, the percentage of the added enzyme affected the size of the resulting cavities as well, thus a cavity was observed in ApnA700. This result suggested that the microstructure changes in the gel network may reduce with an increase in the enzyme ratio. The ratio of 800 µL ApnA/100 mL soymilk formed an interconnected gel matrix with regular distribution with almost invisible cavities compared with lower and higher concentrations (ApnA700 and ApnA900). In turn, the thermal pretreatment and the increased coagulation time might encourage this irregular structure. On the other hand, the gel network coagulated using the reduction of pH showed a weaker gel due to an accelerated acidification. Tofu produced from $MgCl_2$ contained a harder and non-uniform curd same as pH3 effectiveness due to rapid coagulation as well, and this result was in line with Li et al. (2013) and Li et al. (2015). In the study by Li et al. (2013),

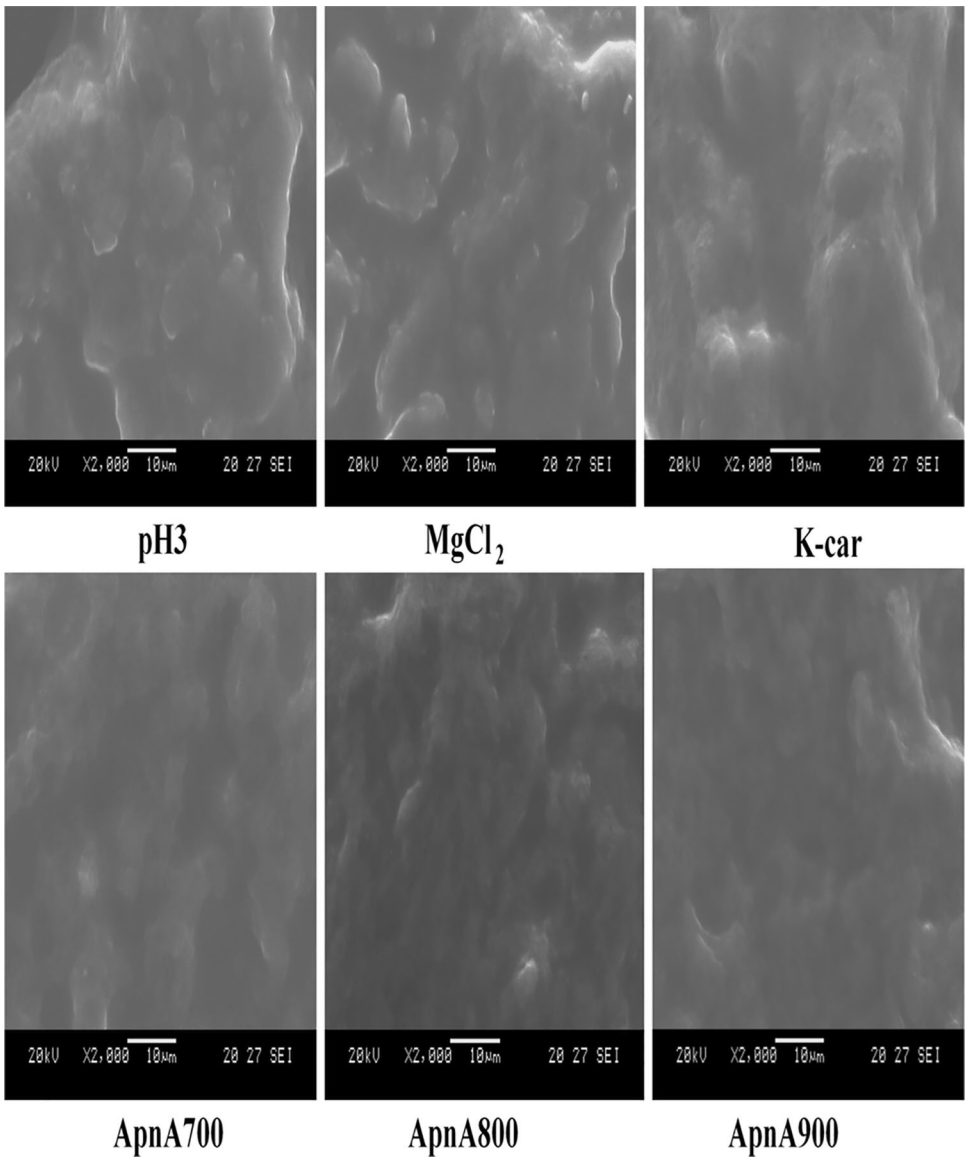

Fig. 7 The electron micrographs of tofu samples prepared from ApnA enzyme at various concentrations and other chemical coagulants

significant distinctions were observed between samples produced with traditional coagulants such as $MgCl_2$ and those using W/O (water-in-oil) coagulants. The samples formed with traditional coagulants exhibited a rough gel consistency with inhomogeneous networks spread over a large area. On the other hand, the samples produced with W/O coagulants displayed smooth and homogenous gel networks. While breaking the curd before squeezing partially disrupted the completed network, this operation had a lesser detrimental impact on the networks of the W/O samples. These networks remained smooth and homogenous even after the breaking process.

Cao et al. (2017) linked the resulted porous and filamentous network with the hydrophobic interaction and their results were in accordance with our findings. The hydrophobic interaction among proteins resulted from the surface charge of soy proteins were preferable through chemical coagulant-induced tofu than that of ApnA-induced tofu. The appearance of a porous and low density network suggested this possibility for chemical induced tofu. On the other hand, the high percentage of water holding capacity and hardness resulting from the enzyme addition reduced these hydrophobic interactions among the gel network. This decrease augmented with the increase of the added enzyme ratio.

Conclusion

Our investigation into the impact of various coagulants, including pH3, MgCl2, and K-carrageenan, and different concentrations of ApnA enzyme, on tofu production revealed distinctive characteristics in terms of yield, composition, texture, thermal stability, water holding capacity, and microstructure. ApnA enzyme, particularly at the concentration of 800 µL/100 mL soymilk, emerged as a promising alternative to traditional chemical coagulants. The results demonstrated that ApnA-treated tofu samples exhibited superior qualities, including higher yield, improved texture with increased hardness and springiness, enhanced thermal stability, lower syneresis values, and a denser, more interconnected gel matrix. The observed modifications in protein structure and interactions, as evidenced by FTIR and fluorescence spectroscopy, contributed to the overall quality enhancement in ApnA-treated tofu. The study not only adds valuable insights into tofu production but also highlights the potential of ApnA enzyme as a key factor for optimizing the quality attributes of tofu. Further research can delve into fine-tuning the enzyme concentration and exploring its applications in diverse tofu formulations to harness its full potential for improved tofu manufacturing.

Supplementary Information The online version contains supplementary material available at https://doi.org/10.1007/s11947-024-03346-8.

Author Contribution Fatma Ali: conceptualization, data curation, formal analysis, writing the original draft, and writing-review and editing. Xuhui Liu: data curation and formal analysis. Sabine Danthine: editing the reviewed draft.

Data Availability Research data are not shared.

Declarations

Conflict of Interest The authors declare no competing interests.

References

Ali, F., Tian, K., & Wang, Z.-X. (2021). Modern techniques efficacy on tofu processing: A review. *Trends in Food Science and Technology, 116*, 766–785.

AOAC. (2000). *Official Methods of Analysis* (17th ed.). Gaithersburg, MD, USA: The Association of Official Analytical Chemists.

Brishti, F. H., Zarei, M., Muhammad, S. K. S., Ismail-Fitry, M. R., Shukri, R., & Saari, N. (2017). Evaluation of the functional properties of mung bean protein isolate for development of textured vegetable protein. *International Food Research Journal, 24*(4), 1595–1605.

Cao, F. H., Li, X. J., Luo, S. Z., Mu, D. D., Zhong, X. Y., Jiang, S. T., Zheng, Z., & Zhao, Y. Y. (2017). Effects of organic acid coagulants on the physical properties and chemical interactions in tofu. *LWT-Food Science and Technology, 85*, 58–65.

Carpenter, J. F., & Crowe, J. H. (1988). The mechanism of cryoprotection of proteins by solutes. *Cryobiology, 25*(3), 244–255.

Carpin´e, D., Dagostin, J. L. A., de Andrade, E. F., Bertan, L. C., & Mafra, M. R. (2016). Effect of the natural surfactant Yucca schidigera extract on the properties of biodegradable emulsified films produced from soy protein isolate and coconut oil. *Industrial Crops and Products, 83*, 364–371.

Gao, X. Q., Kang, Z. I., Zhang, W. G., Li, Y. P., & Zhou, G. H. (2015). Combination of κ-carrageenan and soy protein isolate effects on functional properties of chopped low-fat pork batters during heat-induced gelation. *Food and Bioprocess Technology, 8*(7), 1524–1531.

Ghosh, S., Cramp, G., & Coupland, J. N. (2006). Effect of aqueous composition on the freeze–thaw stability of emulsions. *Colloids and Surfaces a: Physicochemical and Engineering Aspects, 272*, 82–88.

Ibrahim, S. G., Ibadullah, W. Z. W., & Saari b, N., & Karim, R. (2021). Functional properties of protein concentrates of KB6 kenaf (Hibiscus cannabinus) seed and its milky extract. *LWT- Food Science and Technology, 135*, 110234.

Ingrassia, R., Palazolob, G. G., Wagnerb, J. R., & Risso, P. H. (2019). Heat treatments of defatted soy flour: Impact on protein structure, aggregation, and cold-set gelation properties. *Food Structure, 22*, 100130.

Joo, K. H., & Cavender, G. R. (2020). Investigation of tofu products coagulated with trimagnesium citrate as a novel alternative to nigari and gypsum: Comparison of physical properties and consumer preference. *LWT-Food Science and Technology, 118*, 108819.

Kanauchi, M., Hatanaka, S., & Shimoyamada, M. (2015). New cheese-like food production from soy milk utility of soy milk curdling yeast. *Food Production and Industry*. https://doi.org/10.5772/60848

Li, J., Qiao, Z., Tatsumi, E., Saito, M., Cheng, Y., & Yin, L. (2013). A novel approach to improving the quality of bittern-solidified tofu by W/O controlled-release coagulant. 2: Using the improved coagulant in tofu processing and product evaluation. *Food and Bioprocess Technology, 6*, 1801–1808.

Li, M., Chen, F., Yang, B., Lai, S., Yang, H., Liu, K., & Bu, G. (2015). Preparation of organic tofu using organic compatible magnesium chloride incorporated with polysaccharide coagulant. *Food Chemistry, 167*, 168–174.

Li, Y., Liu, B., Jiang, L., Regenstein, J. M., Jiang, N., Poias, V., et al. (2019). Interaction of soybean protein isolate and phosphatidylcholine in nanoemulsions: A fluorescence analysis. *Food Hydrocolloids, 87*, 814–829.

Marangon, M., Van Sluyter, S. C., Robinson, E. M. C., et al. (2012). Degradation of white wine haze proteins by Aspergillopepsin I and II during juice lash pasteurization. *Food Chemistry, 135*, 1157–1165.

Masek, A., Chrzescijanska, E., Kosmalska, A., & Zaborski, M. (2014). Characteristics of compounds in hops using cyclic voltammetry, UV-VIS, FTIR and GC-MS analysis. *Food Chemistry, 156*, 353–361.

Niu, D., Tian, X., Mchunu, N. P., et al. (2017). Biochemical characterization of three Aspergillus niger β-galactosidases. *Electron Journal of Biotechnology, 27*, 37–43.

Phuhongsung, P., Zhang, M., & Devahastin, S. (2020). Influence of surface pH on color, texture and flavor of 3D printed composite mixture of soy protein isolate, pumpkin, and beetroot. *Food and Bioprocess Technology*. https://doi.org/10.1007/s11947-020-02497-8

Premjit, Y., & Mitra, J. (2021). Optimization of electrospray-assisted microencapsulation of probiotics (Leuconostoc lactis) in soy protein isolate-oil particles using Box-Behnken experimental design. *Food and Bioprocess Technology*. https://doi.org/10.1007/s11947-021-02670-7

Qi, B., Ding, J., Wang, Z., Li, Y., Ma, C., Chen, F., et al. (2017). Deciphering the characteristics of soybean oleosome-associated protein in maintaining the stability of oleosomes as affected by pH. *Food Research International, 100*, 551–557.

Qin, X.-S., Chen, S.-S., Li, X.-J., Luo, S.-Z., Zhong, X.-Y., Jiang, S.-T., Zhao, Y. Y., & Zheng, Z. (2017). Gelation properties of transglutaminase-induced soy protein isolate and wheat gluten mixture with ultrahigh pressure pretreatment. *Food and Bioprocess Technology*. https://doi.org/10.1007/s11947-017-1864-9

Rekha, C. R., & Vijayalakshmi, G. (2013). Influence of processing parameters on the quality of soy curd (tofu). *Journal of Food Science and Technology, 50*(1), 176–180.

Shen, Y. R., & Kuo, M. I. (2017). Effects of different carragenan types on the rheological and water holding properties of tofu. *LWT—Food Science and Technology, 78*, 122–128.

Shen, Y. R., & Kuo, M. I. (2014). Changes in the states of protein and water and texture of calcium sulfate tofu during storage. *Fu Jen Journal of Human Ecology, 20*(2), 41–57.

Song, P., Cheng, L., Tian, K., Zhang, M., Mchunu, N. P., Niu, D., Singh, S., Prior, B., & Wang, Z. X. (2020). Biochemical characterization of two new *Aspergillus niger* aspartic proteases. *3 Biotech.* https://doi.org/10.1007/s13205-020-02292-4

Stanojevic, S. P., & Bara´c, M. B., Pe˘si´c, M. B., & Vucelic-Radovic, B. V. (2020). Protein composition and textural properties of inulin-enriched tofu produced by hydrothermal process. *LWT-Food Science and Technology, 126*, 109309.

Su, Y., Dong, Y., Niu, F., Wang, C., Liu, Y., & Yang, Y. (2015). Study on the gel properties and secondary structure of soybean protein isolate/egg white composite gels. *European Food Research and Technology, 240*(2), 367–378.

Sun, D., Li, T., Ma, L., Zhang, F., Li, A., & Jiang, Z. (2019). Effect of selective thermal denaturation and glycosylation on the textural properties and microstructure of vegetable tofu. *Journal of Food Process Engineering, 42*(4), 13001.

Sun-Waterhouse, D., Zhao, M., & Waterhouse, G. (2014). Protein modification during ingredient preparation and food processing: Approaches to improve food processability and nutrition. *Food and Bioprocess Technology, 7*, 1853–1893.

Tang, C. H. (2007). Effect of thermal pretreatment of raw soymilk on the gel strength and microstructure of tofu induced by microbial transglutaminase. *LWT-Food Science and Technology, 40*, 1403–1409.

Theron, L. W., & Divol, B. (2014). Microbial aspartic proteases: Current and potential applications in industry. *Applied Microbiology and Biotechnology, 98*, 8853–8868.

Ullah, I., Hu, Y., You, J., Yin, T., Xiong, S., Din, Z. U., et al. (2019). Influence of okara dietary fiber with varying particle sizes on gelling properties, water state and microstructure of tofu gel. *Food Hydrocolloids, 89*, 512–522.

Vivian, J. T., & Callis, P. R. (2001). Mechanisms of tryptophan fluorescence shifts in proteins. *Biophysical Journal, 80*(5), 2093–2109.

Wang, F., Meng, J., Sun, L., Weng, Z., Fang, Y., Tang, X., et al. (2020). Study on the tofu quality evaluation method and the establishment of a model for suitable soybean varieties for Chinese traditional tofu processing. *LWT-Food Science & Technology, 117*, 108441.

Wang, P., Xu, L., Nikoo, M., Ocen, D., Wu, F., Yang, N., & Xu, X. M. (2014a). Effect of frozen storage on the conformational, thermal and microscopic properties of gluten: Comparative studies on gluten-, glutenin- and gliadin-rich fractions. *Food Hydrocolloids, 35*(3), 238–246.

Wang, Z., Li, Y., Jiang, L., Qi, B., & Zhou, L. (2014b). Relationship between secondary structure and surface hydrophobicity of soybean protein isolate subjected to heat treatment. *Journal of Chemistry, 2014*, 1–10.

Xu, M., Cui, Z., Zhao, L., Hu, S., Zong, W., & Liu, R. (2018). Characterizing the binding interactions of PFOA and PFOS with catalase at the molecular level. *Chemosphere, 203*, 360–367.

Xue, F., Gu, Y., Wang, Y., Li, C., & Adhikari, B. (2019). Encapsulation of essential oil in emulsion based edible films prepared by soy protein isolate-gum acacia conjugates. *Food Hydrocolloids, 96*, 178–189.

Zhang, H., Li, L., Tatsumi, E., & Isobe, S. (2005). High-pressure treatment effects on proteins in soy milk. *Lebensm-Wiss.u-Technol, 38*, 7–14.

Zhang, H., Li, L., Tatsumi, E., & Kotwal, S. (2003). Influence of high pressure on conformational changes of soybean glycinin. *Innovative Food Science and Emerging Technologies, 4*(3), 269–275.

Zhang, L., Zhang, F., & Wang, X. (2016). Changes of protein secondary structures of pollock surimi gels under high-temperature (100 °C and 120 °C) treatment. *Journal of Food Engineering, 171*, 159–163.

Zhang, Q., Wang, C., Li, B., Li, L., Lin, D., Chen, H., Liu, Y., Li, S., Qin, W., Liu, J., Liu, W., & Yang, W. (2019). Research progress in tofu processing: From raw materials to processing conditions. *Critical Reviews in Food Science and Nutrition, 58*(9), 1448–1467.

Zhao, H., Wang, Y., Li, W., Qin, F., & Chen, J. (2016). Effects of oligosaccharides and soy soluble polysaccharide on the rheological and textural properties of calcium sulfate-induced soy protein gels. *Food and Bioprocess Technology*. https://doi.org/10.1007/s11947-016-1826-7

Zheng, L., Teng, F., Wang, N., Zhang, X.-N., Regenstein, J. M., Liu, J.-S., et al. (2019). Addition of salt ions before spraying improves heat-and cold-induced gel properties of soy protein isolate (SPI). *Applied Sciences, 9*(6), 1076.

Zheng, L., Wang, Z.-J., Kong, Y., Ma, Z., Wu, C., Regenstein, J. M., Teng, F., & Li, Y. (2021). Different commercial soy protein isolates and the characteristics of Chiba tofu. *Food Hydrocolloids, 110*, 106115.